



# Bio-economic Dynamics of African Swine Fever: Optimal Control of Transmission and Economic Resource Allocation

Oussama Lazaar<sup>1</sup> and Mustapha Serhani<sup>2</sup>

<sup>1</sup> SIEDD Laborator, Private Univeristy of Fez,  
Lotissement Quaraouiyne Route Ain Chkef, Fez, 30000, Fez-Meknes, Morocco  
lazaar@upf.ac.ma,

<sup>2</sup> Team TSAN, Laboratory TSI, University Moulay Ismail,  
Meknes, 50000, Fez-Meknes, Morocco  
m.serhani@umi.ac.ma

**Abstract.** This paper develops an optimal control model to address the fundamental trade-off between the economic stability of the South Korean pig industry and the transmission of African Swine Fever Virus (ASFV). Therefore, the main objective is to identify the intervention strategies that, during outbreak periods, optimally balance aggressive disease mitigation with the preservation of sectoral economic capital. To achieve this, we formulate a coupled host–vector epidemiological model integrated with a dynamic economic-capital variable, enabling simultaneous analysis of biological transmission and economic resilience. The model incorporates three control measures, which are vaccination, isolation/treatment, and vector control, while explicitly accounting for their implementation costs and long-term economic consequences. Using Pontryagin’s Maximum Principle, we were able to identify intervention strategies that minimize the infected population while simultaneously maximizing the trajectory of economic capital, thereby guaranteeing the long-term sustainability of the industry. These results are reinforced by numerical simulations, which demonstrate that coordinated and optimally timed interventions significantly outperform constant-effort policies.

**Keywords:** African swine fever, mathematical epidemiology, optimal control, Pontryagin’s Maximum Principle, economic impact, cost-effectiveness analysis, South Korea case study, nonlinear dynamical systems

## 1 Introduction

African swine fever virus (ASFV) is a highly contagious viral disease affecting domestic and wild swine, characterized by near 100% mortality and the absence of a commercially viable cure [8, 10]. Beyond direct mortality and culling, its rapid spread triggers severe disruptions in national pig industries and global pork markets, leading to cascading effects on farm incomes, trade, and food security.

Since 2019, South Korea has faced a persistent ASFV outbreak involving both domestic farms and wild boar populations [8, 4]. While intensive surveillance and biosecurity have largely blocked between-farm transmission, the virus continues to migrate

southward through wild boar populations along mountain ranges, posing a constant threat to the national pork sector [5]. This ongoing crisis confirms the urgent need for intervention strategies that are not only epidemiologically effective but also economically sustainable over time.

Mathematical models have become indispensable tools for evaluating these control options. Recent literature has evolved from basic compartmental dynamics to more complex frameworks incorporating fractional derivatives, host-vector reservoirs, and environmental persistence [11, 2, 9]. While previous studies have utilized optimal control to balance suppression costs with biosecurity timing [1, 6], they often treat economic impacts as static costs rather than dynamic variables. Furthermore, while the importance of early intervention has been well-documented [1], many models remain abstract or fail to capture the specific geographical and industrial pressures of the South Korean context.

In response to the ongoing threat of African Swine Fever (ASF) to the South Korean pig industry, this study develops a bioeconomic modeling system to identify intervention strategies that simultaneously control disease transmission and preserve economic stability. The proposed model couples host–vector epidemiological dynamics with an economic-capital variable, allowing the joint evolution of infection and sectoral wealth to be analyzed. Within this investigation, vaccination, treatment/isolation, and vector control are introduced as time-dependent control variables. An optimal control formulation is then used to determine intervention policies that balance epidemiological effectiveness with economic sustainability.

This work provides several novel contributions to the ASF modeling literature. Most notably, the transmission rate is treated as an adaptive parameter that responds to infection conditions and control efforts, enabling the model to capture feedback between intervention intensity and disease propagation. In addition, the explicit inclusion of an economic-capital state variable allows the framework to represent the dynamic impact of disease and mitigation strategies on the financial resilience of the sector. By integrating adaptive epidemiological dynamics with economic evolution, the model offers a unified approach for evaluating both biological and economic outcomes of disease control policies.

The remainder of the paper is organized as follows: First, we formulate a compartmental host–vector model describing the interaction between susceptible, infected, and vaccinated host populations and the vector reservoir, together with an equation governing capital evolution. The optimal control problem is then defined, where the objective functional accounts for infection-related losses, intervention costs, and economic performance (2.1). The necessary optimality conditions are derived using Pontryagin’s Maximum Principle, and the resulting system is solved numerically to obtain the optimal control profiles (2.2). Finally, numerical simulations are presented to illustrate the impact of optimal intervention strategies and to highlight their implications for disease management and economic stability (3).

## 2 Optimal Control Problem

### 2.1 Formulation of the Problem

We consider a deterministic compartmental model describing the transmission dynamics of African swine fever virus (ASFV) within a host population (pigs) and its interaction with a vector (ticks) reservoir [6, 9]. The host population is organized into susceptible, infected, and vaccinated compartments; on the other hand, the vector population is classified into susceptible and infected classes. In addition to the epidemiological states, our model incorporates a time-dependent transmission rate among hosts [3], as well as public health mitigation and economic capital variables. The inclusion of this last variable allows for a formal correlation between disease dynamics and economic outcomes, specifically capturing the dynamic trade-off between the escalating costs of disease control and the preservation of livestock productivity. Moreover, three time-dependent control functions are introduced: vaccination or protection of susceptible hosts, treatment or isolation of infected hosts, and vector control (pesticides, for example) [7, 6].

Disease transmission occurs through direct host-to-host contact and indirect host-vector interactions [9]. The first one is represented through a rate that evolves dynamically in response to infection prevalence and control efforts, reflecting behavioral, policy-driven, and intervention-induced changes in contact patterns [3]. Other essential states are modeled to capture the financial revenue resulting from this pandemic, which are economic environment mitigation and invested capital as they are influenced by disease prevalence, vaccination coverage, and control-associated costs.

The model state variables are defined as follows:  $S_P$ ,  $I_P$ , and  $V_P$  denote the susceptible, infected, and vaccinated host populations, respectively; also, the total host population is denoted by  $N$ , while  $S_T$  and  $I_T$  represent the susceptible and infected vector or environmental compartments. The variable  $\beta_1$  denotes the effective transmission rate, that evolves dynamically in response to infection prevalence and intervention efforts. Additionally, the variables  $M$  and  $K$  describe the state of public health mitigation and capital progress, respectively.

The result coupled controlled system of ordinary differential equations is given by:

$$\left\{ \begin{array}{l} \frac{dS_P}{dt} = \Lambda_P - \mu_P S_P - (1 - v(t)) \left( \beta_1 \frac{S_P I_P}{N} + \beta_2 \frac{S_P I_T}{N} \right) + \tau(t) I_P \\ \frac{dI_P}{dt} = (1 - v(t)) \left( \beta_1 \frac{S_P I_P}{N} + \beta_2 \frac{S_P I_T}{N} \right) - (\mu_P + \delta + \alpha + \tau(t)) I_P \\ \frac{dV_P}{dt} = v(t) S_P + \alpha I_P - \mu_P V_P \\ \frac{dS_T}{dt} = \Lambda_T - \mu_T S_T - \beta_3 \frac{S_T I_P}{N} - \pi(t) S_T \\ \frac{dI_T}{dt} = \beta_3 \frac{S_T I_P}{N} - \mu_T I_T - \pi(t) I_T \\ \frac{d\beta_1}{dt} = \eta - \rho I_P - \gamma(\beta_1 - \beta) - \gamma_V v(t) - \gamma_T \tau(t) \\ \frac{dM}{dt} = d + m I_P - g_V V_P - g_M M - g_K K \\ \frac{dK}{dt} = C_V V_P + C_S S_P - C_I I_P - f_K K - g_0 M \end{array} \right. \quad (1)$$

For the parameters,  $\Lambda_P$  and  $\Lambda_T$  represent recruitment rates into the host and vector populations, while  $\mu_P$  and  $\mu_T$  denote natural mortality rates. The parameters  $\beta_2$  and  $\beta_3$  define the transmission between hosts and vectors [9]. Disease-induced mortality and

recovery or protection are captured by  $\delta$  and  $\alpha$ , respectively [6]. The time-dependent control functions  $v$ ,  $\tau$ , and  $\pi$  correspond to vaccination, treatment or isolation of infected hosts, and pesticide or environmental precautions, respectively [7, 6]. Additional parameters characterize the responsiveness of transmission rate, mitigation, and capital (see Table 1).

Table 1: Model parameters and their biological or economic interpretations.

Parameter	Description	Unit
$\eta$	Baseline transmission input rate	day <sup>-2</sup>
$\rho$	Reduction rate of transmission due to infection prevalence	pigs <sup>-1</sup> ·day <sup>-1</sup>
$\gamma$	Relaxation rate of $\beta_1(t)$ toward baseline $\beta$	day <sup>-1</sup>
$\beta$	Baseline transmission rate	day <sup>-1</sup>
$\gamma_V$	Impact of vaccination on transmission reduction	day <sup>-1</sup>
$\gamma_T$	Impact of treatment/isolation on transmission reduction	day <sup>-1</sup>
$d$	Baseline public health mitigation input	mitigation units·day <sup>-1</sup>
$m$	Effect of infection prevalence on mitigation intensity	mitigation units·pigs <sup>-1</sup> ·day <sup>-1</sup>
$g_V$	Reduction of mitigation due to vaccination coverage	mitigation units·pigs <sup>-1</sup> ·day <sup>-1</sup>
$g_M$	Natural decay rate of mitigation level	day <sup>-1</sup>
$g_K$	Effect of economic development on mitigation	day <sup>-1</sup>
$C_V$	Contribution of vaccinated hosts to economic development	economic units·pigs <sup>-1</sup> ·day <sup>-1</sup>
$C_S$	Contribution of susceptible hosts to economic development	economic units·pigs <sup>-1</sup> ·day <sup>-1</sup>
$C_I$	Economic loss due to infected hosts	economic units·pigs <sup>-1</sup> ·day <sup>-1</sup>
$f_K$	Natural depreciation rate of economic capital	day <sup>-1</sup>
$g_0$	Economic cost associated with mitigation	economic units·(mitigation·day) <sup>-1</sup>

The objective of the optimal control problem is to identify time-dependent intervention strategies that effectively suppress disease transmission while preserving economic performance and limiting the cost of public health responses. Thus, we aim to minimize the cost functional  $\mathcal{J}$  by determining the optimal control functions  $v^*(t)$ ,  $\tau^*(t)$ , and  $\pi^*(t)$  that minimize intensive mitigation and control costs while rewarding higher levels of capital development.

Intuitively, the objective functional  $\mathcal{J}$  serves as a dynamic balancing mechanism between epidemiological safety and sectoral solvency. By assigning a negative weight to the squared capital variable ( $-A_1K(t)^2$ ), the model treats economic growth as a benefit that offsets the total cost of the outbreak. Conversely, the inclusion of the mitigation term ( $A_2M(t)^2$ ) reflects the socio-economic strain and logistical burden placed on the industry when public health measures are active. This formulation ensures that the optimal strategy is not merely the one that kills the virus fastest, but the one that preserves the long-term productive capacity of the South Korean pig industry.

Quadratic cost terms are assigned to the vaccination, treatment or isolation, and vector control functions to represent increasing marginal costs—reflecting the reality that as an intervention scales up, the resources required to reach the next unit of the population become increasingly expensive. Finally, terminal penalty terms are included to prevent short-termism, ensuring that the infection is not just suppressed during the study period but remains at a controlled level with sufficient protection coverage at the final time  $T$ . This identifies the intervention protocols that carefully govern African

swine fever while diminishing adverse economic impacts. Under this consideration, we define the objective function as follows:

$$\mathcal{J} = \int_0^T [-A_1(K(t))^2 + A_2(M(t))^2 + \omega_1 v^2(t) + \omega_2 \tau^2(t) + \omega_3 \pi^2(t)] dt + E_1 I_P(T)^2 + E_2 (V(T) - V_{eq})^2$$

We now formulate the problem within an optimal control structure. Let  $W^{1,1}([0, T], \mathbb{R}_+)$  denotes the space of absolutely continuous functions on  $[0, T]$  taking values in  $\mathbb{R}_+$ , and define the state space by  $\mathcal{S} = W^{1,1}([0, T], \mathbb{R}_+)^8$ . The set of admissible controls is given by  $\mathcal{A} = \mathcal{P}\mathcal{C}([0, T], \mathbb{U})$ , where  $\mathcal{P}\mathcal{C}$  denotes the space of piecewise continuous functions and  $\mathbb{U} = [0, \bar{v}] \times [0, \bar{\tau}] \times [0, \bar{\pi}]$  is the set of controls constraints, where  $\bar{v}$ ,  $\bar{\tau}$  and  $\bar{\pi}$  are positive constants.

The Lagrangian and terminal cost functions are defined, respectively, as

$$L(X, U) = -A_1 x_8^2 + A_2 x_7^2 + \omega_1 u_1^2(t) + \omega_2 u_2^2(t) + \omega_3 u_3^2(t),$$

and

$$\Phi(X(T)) = E_1 x_2(T)^2 + E_2 (x_3(T) - V_{eq})^2,$$

where  $X = (x_1, \dots, x_8) \in \mathcal{D}$  and  $U = (u_1, u_2, u_3) \in \mathbb{U}$ , with  $\mathcal{D} \subset \mathbb{R}_+^8$  is the admissible domain.

Under these definitions, the optimal control problem consists of minimizing the cost functional

$$\mathcal{J}(X, U) = \min_{(X, U) \in \mathcal{S} \times \mathcal{A}} \left\{ \int_0^T L(X(t), U(t)) dt + \Phi(X(T)) \right\}, \tag{2}$$

subject to the controlled dynamical system

$$\begin{cases} \frac{dX}{dt} = f(X(t), U(t)), & t \in [0, T], \\ X(0) = X_0, \end{cases} \tag{3}$$

where  $X = (S_P, I_P, V_P, S_T, I_T, \beta_1, M, K)^T$ ,  $U = (v, \tau, \pi)$ , with  $f = (f_{S_P}, f_{I_P}, f_{V_P}, f_{S_T}, f_{I_T}, f_{\beta_1}, f_M, f_K)^T$ , and  $X_0 = (S_P^0, I_P^0, V_P^0, S_T^0, I_T^0, \beta_1^0, M^0, K^0) \in \mathcal{D}$ .

### 2.2 Optimality conditions

This section is devoted to the derivation of the necessary optimality conditions associated with problem (2)–(3) by means of Pontryagin’s Maximum Principle. From a policy-making perspective, the optimal controls represent time-varying policy intensities, dictating how the effort allocated to vaccination, isolation, and vector control should be scaled up or down at each stage of the outbreak to achieve the most cost-effective result. To this end, we introduce the Hamiltonian function defined by :

$$H(X, U, P, p_0) = P \cdot f(X, U) - p_0 L(X, U),$$

for all  $X = (x_1, \dots, x_8) \in \mathcal{D}$ ,  $U = (u_1, u_2, u_3) \in \mathbb{U}$ ,  $P = (p_1, \dots, p_8) \in \mathbb{R}^8$ , and  $p_0 \in \mathbb{R}$ , where the admissible domain  $\mathcal{D}$  is specified in the previous section.

Let  $(X^*, U^*) \in \mathcal{S} \times \mathcal{A}$  denote an optimal state–control pair for problem (2)–(3). Then, according to Pontryagin’s Maximum Principle, there exists an adjoint vector  $z = (z_1, \dots, z_8) \in W^{1,1}([0, T], \mathbb{R})^8$  and a scalar  $p_0 \in \mathbb{R}$ , not both zero, such that the following conditions hold for almost every  $t \in [0, T]$ :

$$\dot{X}^*(t) = \partial_p H(X^*(t), U^*(t), z(t), p_0), \tag{4}$$

$$\dot{z}(t) = -\partial_X H(X^*(t), U^*(t), z(t), p_0), \tag{5}$$

$$H(X^*(t), U^*(t), z(t), p_0) = \max_{U \in \mathbb{U}} H(X^*(t), U, z(t), p_0), \tag{6}$$

$$z(T) = -p_0 \nabla \Phi(X^*(T)). \tag{7}$$

Here,  $\partial_X$  and  $\partial_p$  denote partial derivatives of the Hamiltonian with respect to the state and adjoint variables, respectively, and  $\nabla$  represents the gradient operator.

These conditions provide a complete characterization of the optimal control strategy and form the basis for the analytical and numerical investigations that follow:

**Theorem 1.** *Let  $(X^*, U^*)$  be an optimal state–control pair associated with problem (2)–(3). Then the optimal control vector  $U^* = (v^*, \tau^*, \pi^*)^T$  is characterized by (10), together with the adjoint system (11) and the corresponding transversality conditions (12).*

*Proof.* Taking the normalized value  $p_0 = 1$ , we can omit it in the variables of the Hamiltonian  $H$ . Hence, the new Hamiltonian is as next:

$$H(X, U, P) = P \cdot f(X, U) - L(X, U).$$

With these considerations, equations (4-7) remain true with the new Hamiltonian and  $p_0 = 1$ .

Remark that, since  $H$  is a concave function with respect to  $u$ , then the Hamiltonian ( $H$ ) admits a global maximum, with respect to the control vector  $U$ . For our purpose, the implementation of PMP leads to an unique optimal control  $U^* = (v^*, \tau^*, \pi^*)$ , that can be handled by comparing  $\tilde{U} = (\tilde{v}, \tilde{\tau}, \tilde{\pi})$ , fulfilling

$$\frac{\partial H}{\partial U}(\tilde{U}) = \begin{pmatrix} \frac{\partial H}{\partial v} \\ \frac{\partial H}{\partial \tau} \\ \frac{\partial H}{\partial \pi} \end{pmatrix} = 0_{\mathbb{R}^3}, \tag{8}$$

with respect the constraints  $\mathbb{U}$ .  
As we have the following,

$$\frac{\partial H}{\partial U} = \begin{pmatrix} 2\omega_1 \tilde{v} \\ 2\omega_2 \tilde{\tau} \\ 2\omega_3 \tilde{\pi} \end{pmatrix} + \begin{pmatrix} z_1 \\ z_2 \\ \vdots \\ z_8 \end{pmatrix}^T \begin{pmatrix} \frac{\partial f_{SP}}{\partial v} & \frac{\partial f_{SP}}{\partial \tau} & \frac{\partial f_{SP}}{\partial \pi} \\ \frac{\partial f_{IP}}{\partial v} & \frac{\partial f_{IP}}{\partial \tau} & \frac{\partial f_{IP}}{\partial \pi} \\ \vdots & \vdots & \vdots \\ \frac{\partial f_K}{\partial v} & \frac{\partial f_K}{\partial \tau} & \frac{\partial f_K}{\partial \pi} \end{pmatrix}$$

The expanded expression for the partial derivative of the Hamiltonian is given by:

$$\frac{\partial H}{\partial U} = \begin{pmatrix} 2\omega_1 \tilde{v} \\ 2\omega_2 \tilde{\tau} \\ 2\omega_3 \tilde{\pi} \end{pmatrix} + \begin{pmatrix} (z_1 - z_2)\beta_1^* \frac{S_P^* I_P^*}{N^*} + z_3 S_P^* - z_6 \gamma \\ (z_1 - z_2)I_P^* - z_6 \gamma \\ -z_4 S_T^* \end{pmatrix}$$

Thus critical point  $\tilde{U}$  verifies:

$$\begin{pmatrix} 0 \\ 0 \\ 0 \end{pmatrix} = \begin{pmatrix} 2\omega_1 \tilde{v} + (z_1 - z_2)\beta_1^* \frac{S_P^* I_P^*}{N^*} + z_3 S_P^* - z_6 \gamma \\ 2\omega_2 \tilde{\tau} + (z_1 - z_2)I_P^* - z_6 \gamma \\ 2\omega_3 \tilde{\pi} - z_4 S_T^* \end{pmatrix}$$

Solving the system above for  $\tilde{U}$  yields to:

$$\begin{pmatrix} \tilde{v} \\ \tilde{\tau} \\ \tilde{\pi} \end{pmatrix} = \begin{pmatrix} \frac{1}{2\omega_1} \left( (z_2 - z_1)S_P^* \frac{(\beta_1 I_P^* + \beta_2 I_T^*)}{N^*} - z_3 S_P^* + z_6 \gamma \right) \\ \frac{(z_2 - z_1)I_P^* + z_6 \gamma}{2\omega_2} \\ \frac{z_4 S_T^* + z_5 I_T^*}{2\omega_3} \end{pmatrix} \tag{9}$$

The overall optimal control  $U^*$  is defined by the constraints on the individual controls:

$$U^* = \begin{pmatrix} \min \{ \bar{v}, \max \{ 0, \tilde{v} \} \} \\ \min \{ \bar{\tau}, \max \{ 0, \tilde{\tau} \} \} \\ \min \{ \bar{\pi}, \max \{ 0, \tilde{\pi} \} \} \end{pmatrix} \tag{10}$$

The adjoint states are obtained from the following system given by

$$\dot{z} = \mathcal{J} \cdot z + \mathcal{X} \tag{11}$$

The Jacobian matrix  $\mathcal{J}$  and  $\mathcal{X}$  are defined as follow:

$$\mathcal{J} = \frac{\partial f}{\partial X} = \left( \frac{\partial f}{\partial S_P} \frac{\partial f}{\partial I_P} \frac{\partial f}{\partial V_P} \frac{\partial f}{\partial S_T} \frac{\partial f}{\partial I_T} \frac{\partial f}{\partial \beta_1} \frac{\partial f}{\partial M} \frac{\partial f}{\partial K} \right)^T$$

$$\mathcal{X} = (0, 0, 0, 0, 0, 0, 2A_2M^*, -2A_1K^*)^T$$

where the row vectors are given by:

$$\frac{\partial f}{\partial S_P} = \left( -\mu_P - (1-v^*) \frac{\beta_1^* I_P^* + \beta_2^* I_T^*}{N^*}, (1-v^*) \frac{\beta_1^* I_P^* + \beta_2^* I_T^*}{N^*}, v^*, 0, 0, 0, 0, C_S \right)^T$$

$$\frac{\partial f}{\partial I_P} = \left( \frac{-(1-v^*)\beta_1^* S_P^*}{N^*} + \tau^*, \frac{(1-v^*)\beta_1^* S_P^*}{N^*} - (\mu_P + \delta + \alpha + \tau^*), \alpha, -\frac{\beta_3^* S_T^*}{N^*}, \frac{\beta_3^* S_T^*}{N^*}, -\rho, m, -C_I \right)^T$$

$$\frac{\partial f}{\partial V_P} = (0, 0, -\mu_P, 0, 0, 0, -g_V, C_V)^T$$

$$\frac{\partial f}{\partial S_T} = \left( 0, 0, 0, -\mu_T - \frac{\beta_3^* I_P^*}{N^*} - \pi^*, \frac{\beta_3^* I_P^*}{N^*}, 0, 0, 0 \right)^T$$

$$\frac{\partial f}{\partial I_T} = \left( \frac{-(1-v^*)\beta_2^* S_P^*}{N^*}, \frac{(1-v^*)\beta_2^* S_P^*}{N^*}, 0, 0, -\mu_T - \pi^*, 0, 0, 0 \right)^T$$

$$\frac{\partial f}{\partial \beta_1} = \left( \frac{-(1-v^*)S_P^* I_P^*}{N^*}, \frac{(1-v^*)S_P^* I_P^*}{N^*}, 0, 0, 0, -\gamma, 0, 0 \right)^T$$

$$\frac{\partial f}{\partial M} = (0, 0, 0, 0, 0, 0, -g_M, -g_0)^T$$

$$\frac{\partial f}{\partial K} = (0, 0, 0, 0, 0, 0, -g_K, -f_K)^T$$

Finally, from (7) we get the next transversality conditions

$$z(T) = \left( -\frac{\partial \Phi}{\partial z_1} - \frac{\partial \Phi}{\partial z_2} - \frac{\partial \Phi}{\partial z_3} - \frac{\partial \Phi}{\partial z_4} - \frac{\partial \Phi}{\partial z_5} - \frac{\partial \Phi}{\partial z_6} - \frac{\partial \Phi}{\partial z_7} - \frac{\partial \Phi}{\partial z_8} \right)^T$$

$$= (0 \ -2E_1 z_2(T) \ -2E_2(z_3(T) - V_{eq}) \ 0 \ 0 \ 0 \ 0 \ 0)^T \tag{12}$$

Thus as  $z(T) = 0$  then we get  $z_2(T) = 0$  and  $z_3(T) = V_{eq}$  such that  $V_{eq} = \frac{\Delta_P \nu}{\mu_P^2}$

### 3 Numerical simulations

To confirm our theoretical findings and assess the effectiveness of the suggested optimal control strategies, we conduct numerical simulations. These simulations are designed to reflect the African Swine Fever outbreak in South Korea. The computational implementation employs a forward-backward sweep method with a time horizon of three years.

The model parameters are collected and calibrated to reflect the epidemiological characteristics and demographic structure observed in South Korean pig farming operations [4, 6].

The pig population dynamics increase by a recruitment rate of  $\Lambda_P = 640$  individuals per day and decline with a natural mortality rate of  $\mu_P = 0.1 \text{ d}^{-1}$ , representing typical commercial herd turnover. The soft tick vector population exhibits a recruitment rate of  $\Lambda_T = 5000$  individuals per day with a natural mortality rate of  $\mu_T = 0.175 \text{ d}^{-1}$ . The disease transmission parameters reflect the multi-step nature of ASF spread: pig-to-pig transmission rate  $\beta_1 = 0.6 \text{ d}^{-1}$ , tick-to-pig transmission  $\beta_2 = 0.3 \text{ d}^{-1}$ , and pig-to-tick transmission  $\beta_3 = 0.2 \text{ d}^{-1}$ . The recovery rate  $\alpha = 0.2 \text{ d}^{-1}$  and disease-induced mortality rate  $\delta = 0.13 \text{ d}^{-1}$  are derived from clinical observations of ASF progression in domestic swine. On the other hand, we summarized the remaining dynamic parameters' values in Table 2.

Table 2: Dynamic transmission and economic parameters

Parameter	Value	Parameter	Value
$\eta$	0.001	$d$	0.3
$\rho$	0.01	$m$	0.0001
$\gamma$	0.05	$g_V$	0.00001
$\gamma_W$	0.03	$g_M$	0.05
$\gamma_T$	0.01	$g_K$	0.0001
$C_V$	0.005	$g_0$	0.01
$C_S$	0.0001	$f_K$	0.02
$C_I$	0.001		

The initial epidemic state corresponds to a moderate farm outbreak scenario. Thus, we initiate the pig population as follows:  $S_P(0) = 10000$  susceptible pigs,  $I_P(0) = 8000$  infected pigs, and  $V_P(0) = 3000$  vaccinated individuals. Next, we start the tick population at  $S_T(0) = 30000$  susceptible and  $I_T(0) = 10000$  infected vectors. Lastly, we allocate the initial mitigation level and the introductory economic capital at  $M(0) = 1.0$  and  $K(0) = 500$ , respectively.

For the objective function, it integrates multiple competing objectives through appropriately scaled weights as presented in Table 3.

Table 3: Cost functional weights

Parameter	Value	Description
$A_1$	0.01	Economic capital weight
$A_2$	1.0	Mitigation cost weight
$\omega_1$	100	Vaccination control cost
$\omega_2$	80	Treatment control cost
$\omega_3$	60	Vector control cost
$E_1$	0.1	Terminal infected penalty
$E_2$	0.001	Terminal vaccination target penalty

Finally, we incorporate the intervention strategies with a maximum feasible implementation rate constrained to  $\bar{v} = 0.35 \text{ d}^{-1}$ ,  $\bar{\tau} = 0.25 \text{ d}^{-1}$ , and  $\bar{\pi} = 0.4 \text{ d}^{-1}$ . The optimal control problem is solved using an iterative forward-backward sweep algorithm with a convergence tolerance of  $\epsilon = 10^{-5}$  and a maximum of 2000 iterations.

The subsequent numerical simulation presents the temporal evolution of state variables optimal control strategies, providing a clear analysis of the optimal management of African Swine Fever outbreaks according to realistic operational and economic constraints in the South Korean agricultural context.

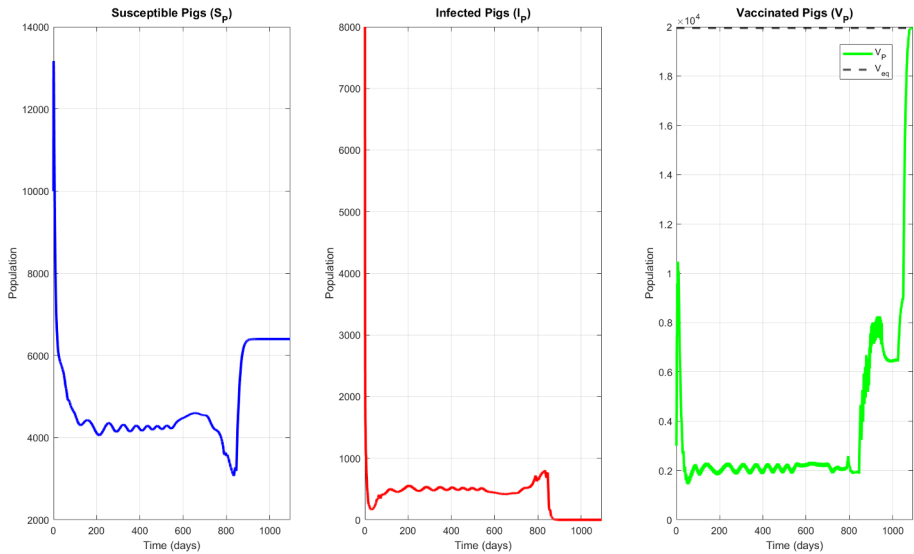


Fig. 1: Pigs Population

The pig population in figure (1) represents the primary economic asset and the main target of the disease. Susceptible pigs ( $S_P$ ) decrease as individuals are transitioned into the vaccinated class, eventually stabilizing once the threat is eliminated. For infected pigs ( $I_P$ ), the control strategies successfully suppress the initial outbreak immediately. However, a low-level endemic presence persists as long as infected ticks are present. Total eradication is achieved shortly after the tick reservoir is cleared (approx. Day 870). The vaccinated compartment ( $V_P$ ) shows a steady baseline during the mitigation phase. Upon reaching the eradication threshold at Day 850, there is a massive surge in  $V_P$ , approaching the equilibrium value  $V_{eq}$  (approx. 20 000), exhibiting that the optimal strategy prioritizes a highly immune domestic herd as the final defense mechanism once active transmission has ceased.

The evolution of the tick population in figure (2) points to the persistence of the environmental reservoir. The susceptible ticks ( $S_T$ ) remain relatively stable with minor oscillations until the eradication of the virus. Following the day 900  $S_T$  experiences a significant recovery and stabilizes at a high level (approx. 27000), representing a

healthy ecosystem free from the pathogen. Next, infected ticks ( $I_T$ ) follow an initial sharp decline from the starting peak; after that, they enter a smoldering state, oscillating between 1000 and 2000 individuals for approximately 800 days. A notable last-gasp spike occurs around Day 830 before the population crashes to zero due to the cumulative effect of controls, especially the pesticide strategy.

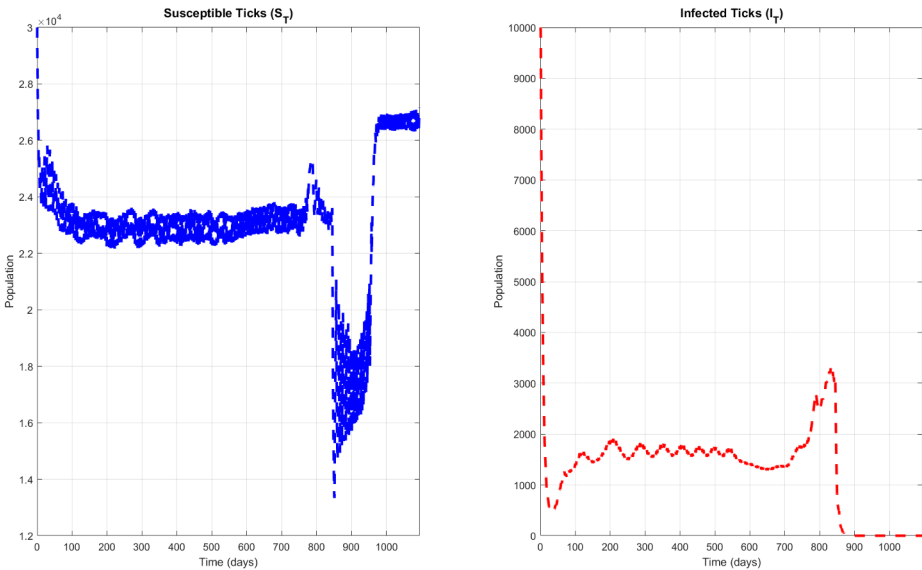


Fig. 2: Ticks Population

The following figure (3) captures the overall performance of the transmission and economic evolution. First, the transmission rate  $\beta_1$  is maintained at zero for the vast majority of the simulation, which is the direct result of the combined optimal control strategies seen in (4). These last effectively block the transmission path. Conceptually, this suggests that the control efforts are sufficient to keep the effective reproductive number well below the threshold of one. However, we notice a sharp rise in the transmission rate after Day 900, peaking at approximately 0.55. This represents the relaxation of restrictive measures. Once the infected populations ( $I_P$  and  $I_T$ ) have been successfully eradicated (as shown in the population figures), the optimizer allows the potential transmission rate to return to its intrinsic levels. Because there are no longer any infected individuals to spread the virus, a high transmission rate no longer poses a risk to the population, allowing the system to stop spending on costly transmission-blocking interventions.

Next, the most critical indicators of policy success are found in the economic capital ( $K$ ) and mitigation level ( $M$ ) graphs. Firstly, we have the Stagnation Period (Days 0–850) in which  $K$  remains relatively flat and low (approx. 500 units) because the high mitigation level ( $M \approx 5.5$ ) effectively consumes the excess value generated by the pig

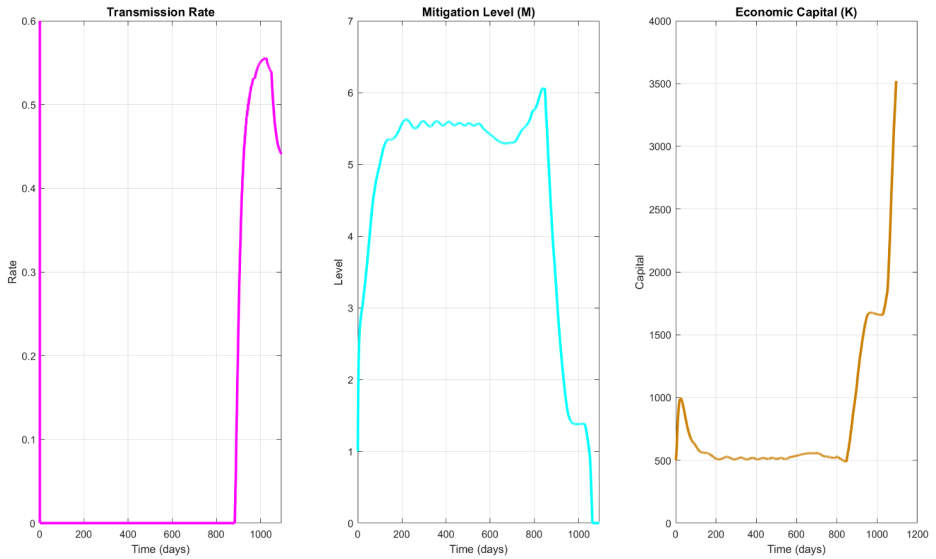


Fig. 3: Transmission and economic evolution

industry. In economic terms, the system is in a loss-mitigation state where all available capital is being reinvested to prevent a total epidemic collapse. This phase demonstrates that early aggressive intervention is a strategic necessity; by front-loading the costs of disease control, the system prevents the virus from becoming an unmanageable, permanent drain on the industry. Following this comes the Economic Explosion (Days 850+). As soon as the infected tick population reaches the eradication threshold, the mitigation level ( $M$ ) drops precipitously, which unlocks the capital that was previously tied up in disease control. Consequently, the economic capital ( $K$ ) undergoes an exponential growth phase, increasing by over 600% (from 500 to 3,500 units) within the final 200 days of the simulation. In sum, this trajectory corroborates the fact that early aggressive intervention generates substantial long-term economic advantages. While the initial stagnation is a period of significant financial sacrifice, it serves as the critical catalyst for the subsequent rapid expansion, demonstrating that proactive suppression is significantly more economically sustainable than a gradual or reactive approach.

In figure 4, the controls illustrate the intensity of effort required to manage ASFV. The optimizer is dynamically responding to small fluctuations in the infected populations to maintain transmission near zero. This is indicated by the chattering or high-frequency switching behavior of vaccination ( $v$ ), treatment ( $\tau$ ), and pesticide control ( $\pi$ ). The high intensity is maintained for nearly 850 days; after that, when eradication is confirmed,  $\tau$  and  $\pi$  are relaxed, while  $v$  maintains a baseline level to provide ongoing preventive protection.

We can also mention that the trajectories for vaccination ( $v$ ), treatment ( $\tau$ ), and pesticide ( $\pi$ ) represent the operational expenditures of the mitigation policy. Firstly, we have the persistent investment such that the high-frequency oscillations and sustained

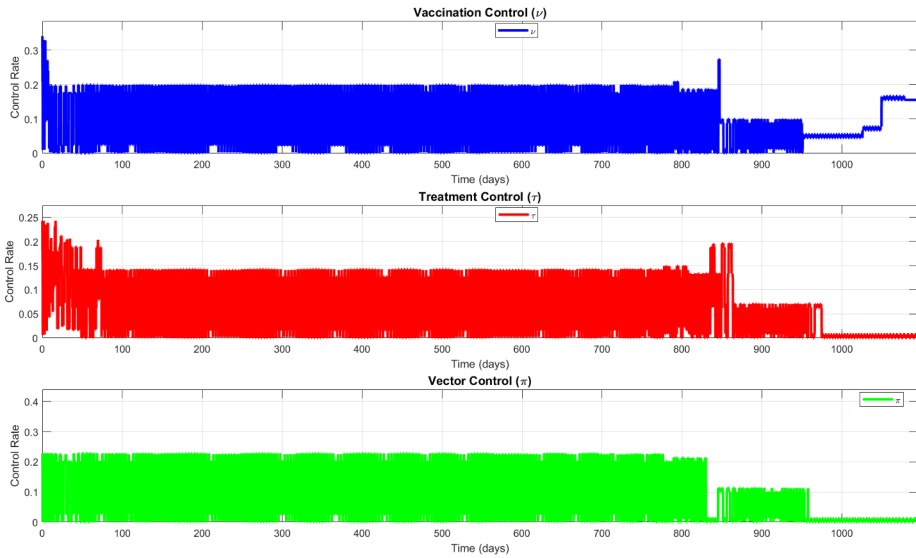


Fig. 4: Control strategies

high levels of all three controls for nearly 2.3 years (850 days) point to the fact that eradication requires a non-wavering financial commitment. While the selective relaxation resulted once the tick reservoir was cleared, the system shifts from active combat to proactive maintenance. Consequently, the subsequent economic surge is primarily driven by the substantial reduction in mitigation spending, which is facilitated by the decrease in  $\tau$  and  $\pi$ .

## 4 limitations

The current study operates under certain structural boundaries defined by the deterministic nature of the model, which provides a rigorous baseline but does not yet account for the stochastic volatility of viral outbreaks or the spatial heterogeneity inherent in localized pig production clusters, such as those in Gyeonggi and Gangwon provinces. Additionally, while the model captures national capital evolution, it remains insulated from the complexities of international market fluctuations and global supply chain instability. Looking forward, this study serves as a foundational outline for several sophisticated extensions; for example, the inclusion of spatial heterogeneity through partial differential equations or the incorporation of stochastic differential equations could provide a more granular representation of environmental uncertainties and seasonal fluctuations.

## 5 Conclusion and perspectives

This research has established a comprehensive optimal control model that illustrates the transmission dynamics of African Swine Fever Virus (ASFV). The theoretical architec-

ture of the model is designed to represent host-vector interactions broadly; however, our analysis is specifically calibrated to the unique ecological and industrial landscape of South Korea. By integrating epidemiological state variables with an economic capital accumulation model, we have demonstrated that the path to long-term agricultural sustainability necessitates a non-trivial period of intensive mitigation. The results confirm that while the domestic pig population can be protected through vaccination and treatment, the permanent success of the control strategy, within the specific parameters of the South Korean sector, depends on the aggressive suppression of the tick-vector reservoir. Our findings indicate that the system undergoes a significant phase of economic stagnation, as available capital is systematically redirected to sustain the high mitigation levels required to keep the transmission rate near zero.

The study's most important contribution is the identification of the economic tipping point that is reached when the environmental reservoir is completely eradicated. Once the infected tick population is eliminated, the system experiences a structural transition where relaxing the high operational costs of vector control and treatment triggers an exponential increase in economic capital that validates the strategy of front-loaded investment. These numerical trajectories are optimized for the South Korean context, such that they highlight a fundamental bio-economic principle that prioritizing absolute eradication over long-term endemic management can unlock remarkable growth. Furthermore, the model illustrates that the subsequent rise in the transmission rate post-eradication does not lead to a resurgence of the disease, as the source of infection has been successfully removed from the environment.

In the end, this work offers a rigorous methodology that outlasts its immediate application; by demonstrating how coordinated, optimally timed interventions can effectively decouple an industry from a viral threat, it establishes a versatile analytical base capable of supporting livestock disease management and policy design across diverse global contexts.

## References

1. Barongo, M.B., Bishop, R.P., Fèvre, E.M., Knobel, D.L., Ssematimba, A.: A mathematical model that simulates control options for African Swine Fever Virus (ASFV). *PLOS ONE* **11**(7), e0158,658 (2016). DOI 10.1371/journal.pone.0158658
2. Chuchard, P., Prathumwan, D., Trachoo, K., Maiaugree, W., Chaiya, I.: The SLI-SC mathematical model of African Swine Fever transmission among swine farms: The effect of contaminated human vector. *Axioms* **11**(7), 329 (2022). DOI 10.3390/axioms11070329
3. Del Valle, S.Y., Mniszewski, S.M., Hyman, J.M.: Modeling the impact of behavior changes on the spread of pandemic influenza. In: *Modeling the Interplay Between Human Behavior and the Spread of Infectious Diseases*, pp. 59–77. Springer (2013). DOI 10.1007/978-1-4614-5474-8\_4
4. Kim, E., Lim, J.S., Pak, S.I.: Mechanistic modelling for African Swine Fever transmission in the Republic of Korea. *Journal of Veterinary Science* **24**(2) (2023). DOI 10.4142/jvs.22262
5. Ko, K.T., Oh, J., Son, C., Choi, Y., Lee, H.: Identifying risk clusters for African Swine Fever in Korea by developing statistical models. *Frontiers in Veterinary Science* **11** (2024). DOI 10.3389/fvets.2024.1416862

6. Kouidere, A., Balatif, O., Rachik, M.: Analysis and optimal control of a mathematical modeling of the spread of African Swine Fever Virus with a case study of South Korea and cost-effectiveness. *Chaos, Solitons & Fractals* **146**, 110,867 (2021). DOI 10.1016/j.chaos.2021.110867
7. Kouidere, A., Balatif, O., Rachik, M.: Fractional optimal control problem for a mathematical modeling of African Swine Fever Virus transmission. *Moroccan Journal of Pure and Applied Analysis* **9**(1), 97–110 (2023). DOI 10.2478/mjpaa-2023-0007
8. Lim, J.S., Andraud, M., Kim, E., Vergne, T.: Three years of African Swine Fever in South Korea (2019–2021): A scoping review of epidemiological understanding. *Transboundary and Emerging Diseases* **2023**(1), 4686,980 (2023). DOI 10.1155/2023/4686980
9. Mugabi, F., Duffy, K.J.: Epidemiological drivers and control strategies for African Swine Fever transmission cycles at a wildlife-livestock interface. *Ecological Modelling* **481** (2023)
10. Niu, X., Shen, D., Bu, Z., Dixon, L.K., Zhao, D.: Hope and hurdles: Unlocking the potential of modified live virus vaccines for African Swine Fever. *Emerging Microbes & Infections* **14**(1), 2572,692 (2025). DOI 10.1080/22221751.2025.2572692
11. Shi, R., Zhang, Y., Wang, C.: Dynamic analysis and optimal control of fractional order African Swine Fever models with media coverage. *Animals* **13**(14), 2252 (2023). DOI 10.3390/ani13142252

**Open Access** This chapter is licensed under the terms of the Creative Commons Attribution-NonCommercial 4.0 International License (<http://creativecommons.org/licenses/by-nc/4.0/>), which permits any noncommercial use, sharing, adaptation, distribution and reproduction in any medium or format, as long as you give appropriate credit to the original author(s) and the source, provide a link to the Creative Commons license and indicate if changes were made.

The images or other third party material in this chapter are included in the chapter's Creative Commons license, unless indicated otherwise in a credit line to the material. If material is not included in the chapter's Creative Commons license and your intended use is not permitted by statutory regulation or exceeds the permitted use, you will need to obtain permission directly from the copyright holder.

